Long-Term Efficacy of Poly(L-lactide-co-ε-caprolactone) Threads With Hyaluronic Acid Nanoparticles: An *In Vivo* Skin Remodeling Study

Pavel A. Burko[1,2], George M. Sulamanidze[3], Dmitriy V. Nikishin[4]

[1] University of Palermo, Palermo, Italy;
[2] Moscow University "Synergy", Moscow, Russia;
[3] APTOS, Tbilisi, Georgia;
[4] Skolkovo Innovation Center, Moscow, Russia

ABSTRACT

BACKGROUND: Modern thread-lifting techniques aim to achieve an immediate mechanical lifting effect and provide a prolonged biostimulatory action directed at remodeling dermal structures.

AIM: This study aimed to perform a histomorphological evaluation of the effects of monofilament P(LA/CL)-HA-nano threads on skin remodeling in a biomedical experiment and compare their outcomes with those of P(LA/CL)-HA threads and intact skin.

METHODS: The study included five clinically healthy female Large White pigs aged 4 months weighing 40 ± 1.2 kg on average. Each animal underwent implantation of two types of threads: P(LA/CL)-HA and P(LA/CL)-HA-nano. Euthanasia of the animals and histomorphological analysis were performed on days 7, 21, 30, 90, and 180. Intact skin was considered the control. The following parameters were assessed: dermal thickness, content of type I and type III collagen fibers, and elastin levels. Histological staining included hematoxylin and eosin, Weigert–Van Gieson, and Picrosirius Red with polarized light analysis. Statistical analysis was conducted using the Wilcoxon signed-rank test. Differences were considered significant at $p < 0.05$.

RESULTS: P(LA/CL)-HA-nano thread implantation resulted in significantly increased dermal thickness (day 180, $p = 0.0431$), increased type I collagen density in the dermis (day 90, $p = 0.0431$) and hypodermis (all time points, $p < 0.05$), and enhanced type III collagen synthesis in the hypodermis from day 21 ($p = 0.0431$). A significant increase in elastin levels in the dermis was observed on days 90 and 180 ($p = 0.0431$). Distinct kinetics of tissue remodeling were noted compared with non-modified P(LA/CL)-HA threads.

CONCLUSION: P(LA/CL)-HA-nano threads exhibit pronounced bioactive properties, promoting structural remodeling of skin tissues.

Keywords: biorevitalization; nonsurgical facelift; hyaluronic acid; skin remodeling; lifting threads.

Долгосрочная эффективность нитей из сополимера пол(L-лактида-со-ε-капролактона) с наночастицами гиалуроновой кислоты: исследование *in vivo* ремоделирования кожи

П.А. Бурко[1,2], Г.М. Суламанидзе[3], Д.В. Никишин[4]

[1] Университет города Палермо, г. Палермо, Италия;

[2] Московский университет «Синергия», г. Москва, Россия;

[3] ООО «АПТОС», г. Тбилиси, Грузия;

[4] Инновационный центр «Сколково», г. Москва, Россия

АННОТАЦИЯ

Актуальность. Современные методы нитевого лифтинга предполагают не только достижение немедленного механического лифтингового эффекта, но и реализацию пролонгированного биостимулирующего действия, направленного на ремоделирование дермальных структур.

Цель исследования. Провести гистоморфологическую оценку влияния монофиламентных нитей P(LA/CL)-ГК-нано на процессы ремоделирования кожи в условиях биомедицинского эксперимента с сопоставлением их эффектов с нитями P(LA/CL)-ГК и интактной кожей.

Методы. В исследование включены пять клинически здоровых самок свиней породы крупная белая, возрастом 4 мес и средней массой тела 40±1,2 кг. Каждому животному имплантировали нити двух типов: P(LA/CL)-ГК и P(LA/CL)-ГК-нано. Выведение животных и гистоморфологический анализ выполняли на 7, 21, 30, 90 и 180-е сутки. В качестве контроля использовали интактные участки кожи. Оценивали толщину дермы, содержание коллагеновых волокон типов I и III, а также уровень эластина. Применяли окраски гематоксилином и эозином, по Вейгерту–Ван Гизону и пикросириусом красным с анализом в поляризованном свете. Статистическую обработку проводили с использованием критерия знаковых рангов Уилкоксона; различия считали статистически значимыми при *p* <0,05.

Результаты. Имплантация нитей P(LA/CL)-ГК-нано сопровождалась достоверным увеличением толщины дермы (к 180-м суткам, *p*=0,0431), повышением плотности коллагена типа I в дерме (90-е сутки, *p*=0,0431) и гиподерме (на всех сроках наблюдения, *p* <0,05), а также усилением синтеза коллагена типа III в гиподерме с 21-х суток (*p*=0,0431). Кроме того, зафиксировано статистически значимое повышение уровня эластина в дерме на 90-е и 180-е сутки (*p*=0,0431). Установлены отличия в кинетике тканевого ремоделирования по сравнению с немодифицированными нитями P(LA/CL)-ГК.

Заключение. Нити P(LA/CL)-ГК-нано проявляют выраженное биоактивное действие, способствуя структурной перестройке кожных тканей.

Ключевые слова: биоревитализация; безоперационная подтяжка лица; гиалуроновая кислота; ремоделирование кожи; лифтинговые нити.

INTRODUCTION

Facial remodeling strategies aimed at mitigating signs of aging have significantly gained popularity over the recent decades. These interventions focus on improving skin elasticity, increasing collagen synthesis, and enhancing skin texture [1].

Since the mid-1990s, the use of various types of nonabsorbable barbed threads, fabricated from different materials, in nonsurgical facial rejuvenation and lifting procedures has been proposed [2, 3]. In 1997, M.A. Sulamanidze developed a polypropylene barbed thread for facial tissue repositioning with aesthetic intent. This technique was named anti-ptosis threads (APTOS). Following the granting of a patent in the Russian Federation in 2002, the author introduced the method internationally, presenting it as an effective tool for addressing age-related changes in facial soft tissues [4].

Since the early 2000s, interest in the use of biodegradable polymers in biomedical technologies has steadily increased [5]. Notably, polydioxanone threads were developed and introduced in South Korea, whereas materials based on poly-L-lactic acid and poly(ε-caprolactone) have gained widespread adoption in Europe, Russia, and the United States [3].

Currently, particular attention is being given to the copolymer poly(L-lactide-co-ε-caprolactone) [P(LA/CL)], which is synthesized from ε-caprolactone and L-lactic acid [6]. Owing to its high biocompatibility, favorable tolerability, and slow biodegradation rate, P(LA/CL) is of particular interest for use in procedures requiring prolonged therapeutic effects [6–8]. P(LA/CL) threads are characterized by a complete biodegradation period of up to 12 months, while promoting active remodeling of the dermal matrix and potentially providing a sustained lifting effect [8]. In vivo experimental study results indicate that, owing to their pronounced collagen-stimulating activity, the effects of P(LA/CL) threads may persist for over 18 months, demonstrating superiority over earlier-generation thread materials [8, 9].

Within thread-based facial rejuvenation techniques, the immediate mechanical properties of the threads that ensure the lifting effect and their ability to support ongoing dermal remodeling processes should be considered. Insufficient regenerative potential may limit the long-term effectiveness of the intervention and negate the clinicians' therapeutic expectations and patients' aesthetic demands [10].

According to the literature, the use of hyaluronic acid (HA) as an adjunct component in thread-lifting procedures is regarded as a clinically justified strategy aimed to enhance therapeutic efficacy and improve clinical outcomes [11–14]. The implementation of this synergistic approach amplifies the lifting effect and significantly decreases the incidence and severity of postoperative complications, which remain a pressing concern in aesthetic medicine [15]. Furthermore, this combination contributes to greater overall treatment effectiveness and increased patient satisfaction [15–18].

In 2019, the development of NAMICA (NAno–MIcro–CApsule) encapsulation technology was initiated; in 2022, it received patent protection [18, 19]. This method was designed to sustain release of HA from the surface of lifting threads by encapsulating it within a biodegradable copolymer. Based on this approach, a new type of lifting thread, P(LA/CL)-HA-nano, was developed, characterized by the incorporation of HA into a nanostructured polymer matrix. To date, no experimental data on the efficacy of these threads have been reported in the scientific literature.

Thus, **this study aimed** to perform a histomorphological evaluation of skin remodeling processes following P(LA/CL)-HA-nano thread implantation in an experimental porcine model. This study included a comparative analysis of their effects on key morphological parameters of the skin, such as dermal thickness, type I and type III neocollagenesis, and elastogenesis, relative to P(LA/CL)-HA threads without nano-encapsulation and intact skin.

METHODS

The animal experimental study was approved by the Local Ethics Committee of the "Center for Preclinical Research LLC" (Penza, Russia; protocol № 5-2023, dated August 23, 2023).

The present study used clinically healthy Large White pigs (n = 5).

Inclusion criteria:

1. Breed: Large White (*Sus scrofa domesticus*)

2. Age: 4 months

3. Body weight: 40 ± 2 kg

4. Sex: female

5. General health status: clinically healthy animals with no signs of somatic, infectious, or traumatic pathology, as confirmed by veterinary examination

6. Adaptation period: a 7-day acclimatization phase in vivarium conditions was implemented prior to the start of the study

Exclusion criteria:

1. Somatic or infectious disorders: presence of clinical signs of disease, external or internal injuries, or pathological abnormalities detected during examination or health monitoring

2. Reproductive status: pregnant or lactating females

3. Experimental history: animals previously subjected to invasive procedures or stress-inducing experimental interventions

The experimental protocol was organized and executed in strict accordance with the provisions of the European Convention for the Protection of Vertebrate Animals Used for Experimental and Other Scientific Purposes (ETS № 123, 1986), the Recommendations of the European Commission 2007/526/EC, and Directive 2010/63/EU of the European Parliament and of the Council of the European Union.

The experiment was conducted according to international standards ISO 10993-1:2018[1] and ISO 10993-2:2022[2]. The animals were housed in a certified vivarium under full compliance with regulatory requirements for the care and use of laboratory animals. The ambient temperature was maintained at $21 \pm 2\,°C$, with relative humidity of 30–60%. The light/dark cycle was set to 12 hours of light and 12 hours of darkness, starting at 07:00 daily. Throughout the housing period, the pigs were provided with standardized pelleted feed tailored to their age and physiological needs and unrestricted access to clean drinking water.

Following a 7-day acclimatization period, each of the five animals was assigned an individual identification number by randomization through a lottery method. The animals underwent implantation of threads into the cutaneous tissue, whereas intact skin areas of the same animals—to which no threads were implanted—served as intra-individual controls. Each animal was randomly assigned to one of five experimental endpoints (days 7, 21, 30, 90, and 180), enabling sequential histomorphological evaluation of tissue changes at different stages of skin remodeling. Thus, the study was designed as a temporal cross-sectional comparison with elements of intra-subject control, without formal division into experimental groups.

The animals received analgesic and anesthetic agents approved for use in veterinary practice[3]. During the induction phase, each pig received intramuscular injection of xylazine at 3 mg/kg (6 mL) and Zoletil® 100 (tiletamine + zolazepam) at 1.75 mg/kg (0.7 mL). Stable levels of anesthesia and analgesia were maintained during the surgical procedure via facemask inhalation anesthesia with isoflurane (3 vol.% for induction and 1.5 vol.% for maintenance) in an oxygen mixture, along with continuous intravenous infusion of propofol at 25 mL/h [20].

To prevent purulent-inflammatory complications, all animals received a single intramuscular injection of the broad-spectrum antibiotic ceftriaxone at 25 mg/kg (1 g in 1 mL for a 40 kg animal), according to the principles of prophylactic antibacterial therapy.

The skin areas on the limbs (both forelimbs and hind limbs) and torso were depilated and disinfected with 70% ethanol prior to surgery to ensure aseptic conditions.

Implantation was performed using a straight 18 G needle, through which five threads of each test variant were inserted into the subcutaneous tissue of each animal. The threads were introduced parallel to the skin surface to ensure optimal integration of the implants. On the right side of each animal's body, five insertion points were established for resorbable P(LA/CL)-HA thread placement; on the left side, five P(LA/CL)-HA-nano threads were implanted following an identical protocol. The implantation sites were covered with sterile adhesive dressings to prevent infectious complications.

Each thread used in the procedure was 15 cm long, had a smooth (non-barbed) surface, and had a USP size of 2-0. All surgical procedures were completed without the occurrence of postoperative complications.

Following thread implantation, tissue harvesting (skin and subcutaneous fat) was conducted at five time points, namely, days 7, 21, 30, 90, and 180, for histological evaluation. A 15 cm section of soft tissue was excised, from which three samples (one from each edge and one from the central region) were collected for subsequent microscopic analysis. The intact skin served as the control.

At the designated endpoint for each animal, euthanasia was performed by intravenous administration of an overdose of sedative–anesthetic agent, followed by exsanguination once deep pharmacological sedation was achieved[2].

The tissue samples were subjected to standard histological processing followed by paraffin embedding [21]. Full-thickness sections measuring 5–7 µm were prepared from each block, with three sections placed per microscope slide. After deparaffinization, the slides were stained using standard histological methods: hematoxylin and eosin, Weigert–Van Gieson (WVG), and Picrosirius Red (SR).

Morphological evaluation of the tissue response to biomaterial implantation was carried out according to the international standard ISO 10993-6:2016[4]. The analysis focused on the following target histological parameters:

1. Dermal thickness, µm

2. Density of type I collagen fibers in the dermis and hypodermis (arbitrary units; pixel intensity)

3. Density of type III collagen fibers in the dermis and hypodermis (arbitrary units; pixel intensity)

4. Density of elastic fibers in the dermis and hypodermis (arbitrary units; pixel intensity)

Notably, additional clarification regarding the histological staining methods employed in this study is warranted. The WVG technique was used to differentiate elastic fibers from collagen fibers. Although SR staining is frequently applied for the detection of amyloid deposits, in the present study, it was adapted for polarized light microscopy to enable visual discrimination between collagen types; type I collagen

[1] GOST R ISO 10993-1-2021 "Biological evaluation of medical devices. Part 1. Evaluation and testing as part of the risk management process." Moscow, 2022. 44 p. (In Russ.)

[2] GOST R ISO 10993-2-2009 "Biological evaluation of medical devices. Part 2. Requirements for handling animals." Moscow, 2010. 16 p. (In Russ.)

[3] State Register of Veterinary Medicines (list of medicinal products that have undergone state registration). (In Russ.) Available at: https://fsvps.gov.ru/files/gosudarstvennyj-reestr-lekarstvennyh-sredstv-dlja-veterinarnogo-primenenija-perechen-lekarstvennyh-preparatov-proshedshih-gosudarstvennuju-registraciju/ Accessed on: June 24, 2025.

[4] GOST R ISO 10993-6-2021 "Evaluation of the biological effect of medical devices. Part 6. Studies of local action after implantation". Moscow, 2021. 34 p. (In Russ.)

appeared strongly birefringent bright red, whereas type III collagen exhibited a greenish hue. Hematoxylin counterstaining was intentionally omitted from the SR-stained sections to avoid interference from nuclear contrast and thus ensure the most accurate assessment of collagen fiber density.

Histological sections were examined with a digital microscope equipped with a 12-megapixel Sony camera under standard and polarized light conditions. Five microphotographs were captured at ×40 magnification for each sample. At ×100 magnification, ten images were obtained, which were evenly distributed between the dermis and hypodermis. The same procedure was applied at ×200 magnification, yielding ten additional micrographs per section, equally representing both skin layers.

Image acquisition and analysis were performed using ImageView v.3.7.7 and HistMorph v.2.3.

Statistical processing of the obtained data was performed using Statistica v.7.0 (StatSoft Inc., USA). Quantitative variables were described with the following parameters: the mean ± standard error of the mean (M ± m), median, interquartile range (25th and 75th percentiles), and minimum and maximum values.

Analysis of changes in the studied parameters over time (within-group analysis) and comparisons between thread types at individual time points were conducted using the Wilcoxon signed-rank test. $P < 0.05$ was considered statistically significant. Values between 0.05 and 0.1 were indicative of a trend toward statistical significance.

RESULTS

Tissue Changes Due to P(LA/CL)–HA-nano Sutures

The most pronounced changes were observed between days 30 and 90, manifested by a consistent increase in dermal thickness and type I collagen content and alterations in the density of type I and type III collagen fibers in the hypodermis ($p = 0.0431$).

Comparative analysis between the baseline (day 7) and final time point (day 180) revealed significant differences in dermal thickness, type I and type III collagen density in the hypodermis, and elastin density in the dermis and hypodermis ($p = 0.0431$). For type III collagen in the dermis, a trend toward statistical significance was noted ($p = 0.0796$). In contrast, changes in type I collagen density in the dermis did not reach statistical significance ($p = 0.2249$).

Comparative Evaluation of P(LA/CL)–HA-nano Sutures Versus P(LA/CL)–HA Sutures and Control Across Histological Parameters

Dermal Thickness

P(LA/CL)-HA-nano vs. Control. The dermal thickness in the P(LA/CL)-HA-nano group was lower than that in the control group (1981.14 ± 89.64 μm) on days 7 and 21. The difference was significant on day 7 (1320.55 ± 87.62 μm; $p = 0.0431$),
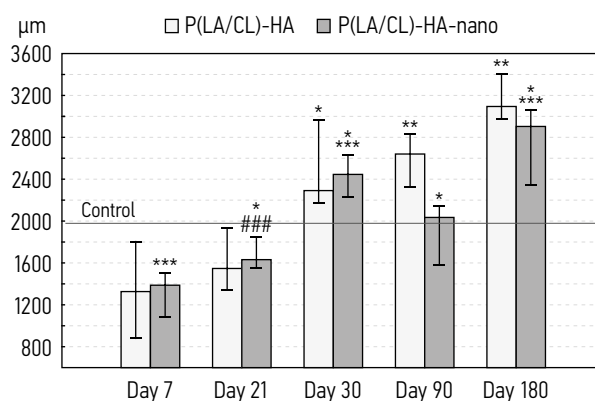
Figure 1. Dermal thickness (μm) (Wilcoxon signed-rank test). Each box plot represents the median and first (Q1) and third (Q3) quartiles. *, Significant difference between study time points. **, Significant difference between thread types. ***, Significant difference between the P(LA/CL)-HA-nano and control groups. ###, Changes between the P(LA/CL)-HA-nano and control reached statistical significance.

whereas a trend toward significance was observed on day 21 (1667.02 ± 59.91 μm; $p = 0.0796$). However, from day 30 to day 180, the dermal thickness values in the P(LA/CL)-HA-nano group exceeded those in the control group, with significant differences recorded on days 30 (2445.41 ± 70.83 μm; $p = 0.0431$) and 180 (2768.61 ± 135.52 μm; $p = 0.0431$).

P(LA/CL)-HA-nano vs. P(LA/CL)-HA. On day 30, dermal thickness in the P(LA/CL)-HA-nano group was greater than that in the P(LA/CL)-HA group. However, by day 90, it had decreased, and on days 90 (1906.78 ± 112.79 μm vs. 2619.65 ± 93.86 μm) and 180 (2768.61 ± 135.52 μm vs. 3044.56 ± 154.96 μm), dermal thickness in the P(LA/CL)-HA-nano group was significantly lower than that in the P(LA/CL)-HA group ($p = 0.0431$).

Figure 1 presents histological data illustrating the dynamics of dermal thickness changes.

Density of Type I Collagen Fibers in the Dermis

P(LA/CL)-HA-nano vs. Control. Throughout the observation period, the level of type I collagen in the dermal layer of the skin in the P(LA/CL)-HA-nano group exceeded that in the control group (71.12 ± 6.22 arbitrary units). A significant difference was observed on day 90 (88.34 ± 1.94 arbitrary units; $p = 0.0431$).

P(LA/CL)-HA-nano vs. P(LA/CL)-HA. On day 7, the level of type I collagen in the dermis was greater in the P(LA/CL)-HA-nano group (80.42 ± 2.18 arbitrary units) than in the P(LA/CL)-HA group (75.26 ± 2.89 arbitrary units); however, this difference was not significant ($p = 0.2249$). At subsequent time points, type I collagen levels in the P(LA/CL)-HA group exceeded those in the P(LA/CL)-HA-nano group; no significant differences were observed, although a strong trend toward significance was noted on day 30 ($p = 0.0796$).

Figure 2 shows the histological data reflecting type I collagen levels in the dermal layer.
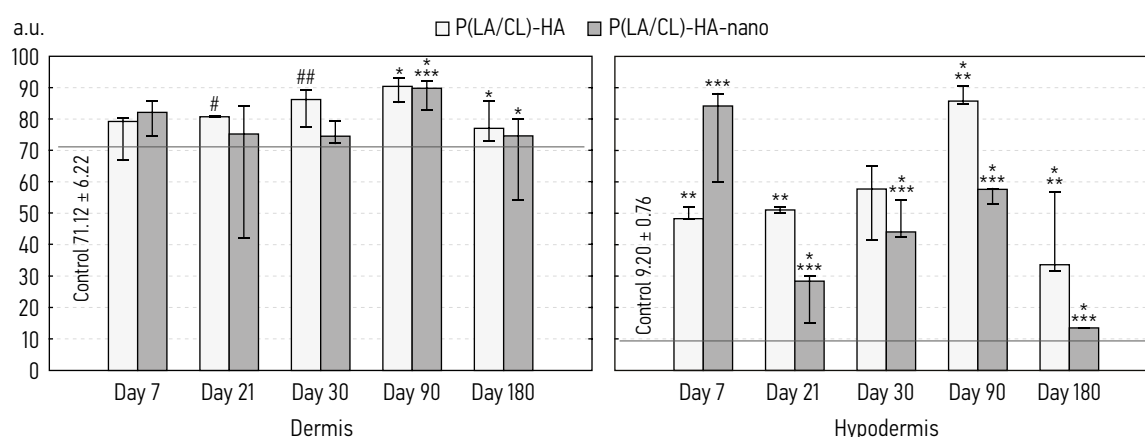
Figure 2. Density of type I collagen fibers in the dermis and hypodermis, arbitrary units (pixel intensity) (a.u.) (Wilcoxon signed-rank test). Each box plot displays the median and first (Q1) and third (Q3) quartiles. *, Significant difference between study time points. **, Significant difference between thread types. ***, Significant difference between the P(LA/CL)-HA-nano and control groups. #, Changes over time reached statistical significance. ##, Difference between thread types reached statistical significance.

Density of Type I Collagen Fibers in the Hypodermis

P(LA/CL)-HA-nano vs. Control. Throughout the observation period, the level of type I collagen in the hypodermis in the P(LA/CL)-HA-nano group consistently exceeded that in the control. At all time points, the differences were significant ($p = 0.0431$).

P(LA/CL)-HA-nano vs. P(LA/CL)-HA. On day 7, the level of type I collagen in the hypodermis was significantly greater in the P(LA/CL)-HA-nano group than in the P(LA/CL)-HA group (70.94 ± 4.92 vs. 42.34 ± 2.64 arbitrary units; $p = 0.0431$). At later time points, the P(LA/CL)-HA group demonstrated greater values than did the P(LA/CL)-HA-nano group, with significant differences observed on days 21 (43.30 ± 2.75 vs. 21.96 ± 2.94), 90 (78.36 ± 1.13 vs. 52.76 ± 2.82), and 180 (37.82 ± 5.16 vs. 12.16 ± 0.51) ($p = 0.0431$). Notably, the P(LA/CL)-HA-nano group exhibited the highest level of type I collagen on day 7 (70.94 ± 4.92), followed by a progressive decrease to its lowest value on day 180 (12.16 ± 0.51). In contrast, the P(LA/CL)-HA group reached its peak on day 90 (78.36 ± 1.13), with a subsequent decrease to a minimum level by day 180 (37.82 ± 5.16).

Figure 2 presents the histological data illustrating type I collagen content in the hypodermal layer.

Density of Type III Collagen Fibers in the Dermis

P(LA/CL)-HA-nano vs. Control. From day 7 to 180, the content of type III collagen in the dermal layer remained consistently lower in the P(LA/CL)-HA-nano group than in the control group (12.18 ± 2.77 arbitrary units; p = 0.0021). Significant differences were found on days 7 (4.84 ± 0.58 arbitrary units) and 30 (4.06 ± 0.71 arbitrary units; $p = 0.0431$), whereas a trend toward significance was noted on day 90 (4.56 ± 1.13 arbitrary units; $p = 0.0796$).

P(LA/CL)-HA-nano vs. P(LA/CL)-HA. From day 7 to 90, the content of type III collagen in the dermis was greater in the P(LA/CL)-HA group than in the P(LA/CL)-HA-nano group, with a trend toward statistical significance observed on day 7 (11.40 ± 2.36 vs. 4.84 ± 0.58 arbitrary units; $p = 0.0796$). In contrast, on day 180, type III collagen levels in the P(LA/CL)-HA-nano group (8.76 ± 2.09 arbitrary units) exceeded those in the P(LA/CL)-HA group (4.06 ± 0.81 arbitrary units); however, the difference did not reach statistical significance ($p = 0.1380$). Notably, type III collagen levels in the P(LA/CL)-HA group steadily decreased over the entire observation period, whereas those in the P(LA/CL)-HA-nano group exhibited a fluctuating pattern: an increase from day 7 to 21 (from 4.84 ± 0.58 to 12.64 ± 5.50 arbitrary units), a decrease from day 21 to 90 (to 4.56 ± 1.13), and a subsequent increase from day 90 to 180 (to 8.76 ± 2.09).

Figure 3 shows the histological data regarding type III collagen content in the dermis.

Density of Type III Collagen Fibers in the Hypodermis

P(LA/CL)-HA-nano vs. Control. Throughout the observation period, the content of type III collagen in the hypodermal layer of the skin in the P(LA/CL)-HA-nano group remained consistently and significantly greater than that in the control (13.70 ± 1.18 arbitrary units; $p = 0.00001$).

P(LA/CL)-HA-nano vs. P(LA/CL)-HA. On day 7, the level of type III collagen in the hypodermis was greater in the P(LA/CL)-HA group (20.78 ± 2.40 arbitrary units) than in the P(LA/CL)-HA-nano group (17.60 ± 3.65 arbitrary units); however, the difference was not significant ($p = 0.5002$). At subsequent time points, the values in the P(LA/CL)-HA-nano group exceeded those in the P(LA/CL)-HA group. Notably, in the P(LA/CL)-HA-nano group, peak levels of type III collagen were observed on days 21 (51.74 ± 2.52) and 180 (51.86 ± 0.61), whereas in the P(LA/CL)-HA group, the peak was recorded only on day 180 (30.90 ± 3.29).

Figure 3 reveals the histological findings related to type III collagen content in the hypodermis.
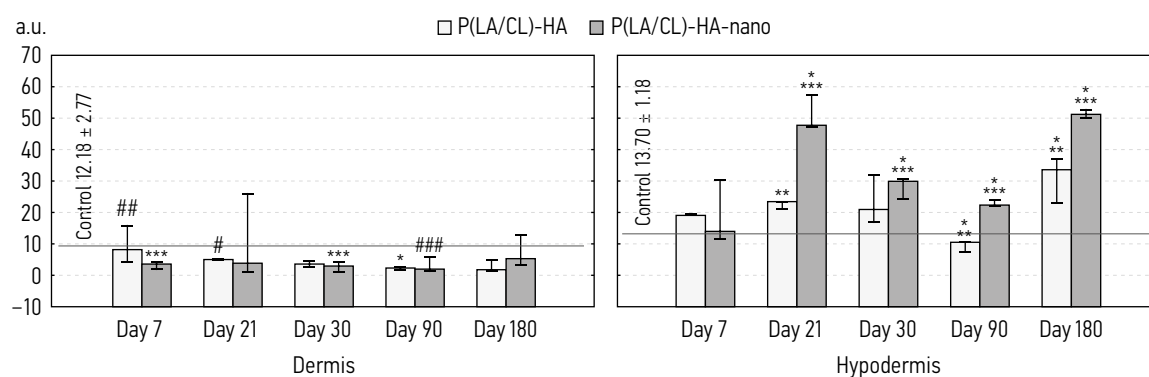
Figure 3. Density of type III collagen fibers in the dermis and hypodermis, arbitrary units (pixel intensity) (a.u.) (Wilcoxon signed-rank test). Each box plot displays the median and first (Q1) and third (Q3) quartiles. *, Significant difference between study time points. **, Significant difference between thread types. ***, Significant difference between the P(LA/CL)-HA-nano group and control group. #, Changes over time reached statistical significance. ##, Difference between thread types reached statistical significance. ###, Changes between the P(LA/CL)-HA-nano and control reached statistical significance.
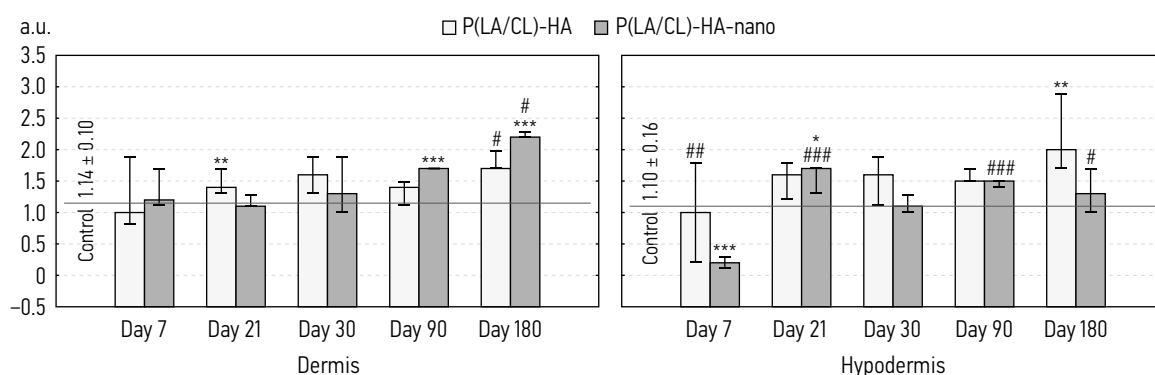
Figure 4. Density of elastic fibers in the dermis and hypodermis, arbitrary units (pixel intensity) (a.u.) (Wilcoxon signed-rank test). Each box plot displays the median and first (Q1) and third (Q3) quartiles. *, Significant difference between study time points. **, Significant difference between thread types. ***, Significant difference between the P(LA/CL)-HA-nano group and control group. #, Changes over time reached statistical significance. ##, Difference between thread types reached statistical significance. ###, Changes between the P(LA/CL)-HA-nano and control reached statistical significance.

Density of Elastic Fibers in the Dermis

P(LA/CL)-HA-nano vs. Control. Elastin levels in the dermis were greater in the P(LA/CL)-HA-nano group on days 7 (1.32 ± 0.11 arbitrary units), 30 (1.42 ± 0.18), 90 (1.70 ± 0.03), and 180 (2.08 ± 0.17) than in the control group (1.10 ± 0.16). Significant differences were observed on days 90 and 180 ($p = 0.0431$). On day 21, the elastin levels were nearly identical to those of the control, with no significant difference detected ($p = 0.8551$).

P(LA/CL)-HA-nano vs. P(LA/CL)-HA. Significant differences in dermal elastin levels between the study groups were observed only on day 21 ($p = 0.0431$), when values in the P(LA/CL)-HA group (1.48 ± 0.07 arbitrary units) were greater than those in the P(LA/CL)-HA-nano group (1.16 ± 0.04). On day 30, the elastin level in the P(LA/CL)-HA group (1.60 ± 0.11) exceeded that in the P(LA/CL)-HA-nano group (1.42 ± 0.18); however, the difference was not significant ($p = 0.2733$). Conversely, on days 7 (1.32 ± 0.11 vs. 1.18 ± 0.20; $p = 0.5002$), 90 (1.70 ± 0.03 vs. 1.44 ± 0.13; $p = 0.1380$), and 180 (2.16 ± 0.22 vs. 1.80 ± 0.06; $p = 0.1056$), elastin levels in the dermis were higher in the P(LA/CL)-HA-nano group than

in the P(LA/CL)-HA group, although none of these differences reached statistical significance.

Figure 4 spresents the histological findings concerning dermal elastin levels.

Density of Elastic Fibers in the Hypodermis

P(LA/CL)-HA-nano vs. Control. On day 7, elastin levels in the hypodermal layer were significantly lower in the P(LA/CL)-HA-nano group (0.18 ± 0.04 arbitrary units) than in the control group (1.10 ± 0.16; $p = 0.0431$). From day 21 onward, the values in the P(LA/CL)-HA-nano group exceeded those in the control group: 1.54 ± 0.10 on day 21, 1.28 ± 0.16 on day 30, 1.52 ± 0.07 on day 90, and 1.32 ± 0.12 on day 180. A trend toward statistical significance was observed on days 21 and 90 ($p = 0.0796$).

P(LA/CL)-HA-nano vs. P(LA/CL)-HA. Differences in hypodermal elastin levels between the study groups were observed only on day 180, when values in the P(LA/CL)-HA group (2.16 ± 0.22 arbitrary units) were significantly greater than those in the P(LA/CL)-HA-nano group (1.32 ± 0.12; $p = 0.0431$). On days 7 and 30, elastin levels were greater

in the P(LA/CL)-HA group (1.32 ± 0.12 on day 7; 1.48 ± 0.16 on day 30) than in the P(LA/CL)-HA-nano group (0.18 ± 0.04 on day 7; 1.28 ± 0.16 on day 30), with a trend toward statistical significance observed on day 7 ($p = 0.0679$). On day 21, elastin levels in the hypodermis were slightly greater in the P(LA/CL)-HA-nano group (1.54 ± 0.10) than in the P(LA/CL)-HA group (1.50 ± 0.11); however, the difference was not significant ($p = 0.7874$).

Figure 4 shows the histological results reflecting the elastin content in the hypodermal layer.

DISCUSSION

In the present study, the dynamics of dermal thickness over a 6-month period were characterized to assess the biological behavior of P(LA/CL)-HA-nano threads.

Between days 7 and 21, the dermal thickness in the P(LA/CL)-HA-nano group was lower than that in the control group (1981.14 ± 89.64 μm). A significant decrease was recorded on day 7 (1320.55 ± 87.62 μm; $p = 0.0431$), and a trend toward significance was observed on day 21 (1667.02 ± 59.97 μm; $p = 0.0796$), which may reflect the mechanical effect induced by thread implantation.

Following the initial decrease, the dermal thickness significantly increased from day 30 (2445.41 ± 70.83 μm) to 180 (2768.61 ± 135.52 μm), with significant differences observed at both time points ($p = 0.0431$ for each), indicating a pronounced remodeling effect. This dynamic may be attributable to the sustained release of HA from the nanoencapsulated form, which promotes collagen synthesis and skin remodeling [22, 23].

Over the 6-month observation period, the dermal thickness in areas treated with P(LA/CL)-HA-nano threads recovered from the initial reduction and exceeded the values recorded in controls. This indicates the capacity of the threads to enhance tissue remodeling and their successful integration into the dermal matrix. The significant differences observed on days 30 and 180 ($p = 0.0431$ for both) emphasize the potential of this thread type to increase dermal thickness and improve the morphofunctional condition of the skin.

A comparison with conventional P(LA/CL)-HA threads revealed that during the early phase (up to day 30), both groups presented comparable dermal thickness values. However, from that point onward, an opposing trend emerged: the dermal thickness in the P(LA/CL)-HA group significantly exceeded that in the P(LA/CL)-HA-nano group throughout the remainder of the observation period. Significant differences were recorded on days 90 (2619.65 ± 93.86 μm vs. 1906.78 ± 112.79 μm) and 180 (3044.56 ± 154.96 μm vs. 2768.61 ± 135.52 μm) ($p = 0.0431$ for both comparisons). These differences may be attributable to variations in biological activity and degradation profiles between the nanoencapsulated and non-modified forms of HA used in the thread composition.

P(LA/CL)-HA-nano threads demonstrated a significant increase in dermal thickness from day 7 (1320.55 ± 87.62 μm)

to 180 (2768.61 ± 135.52 μm; $p = 0.0431$), indicating their potential for use in areas requiring tissue volumization and enhanced structural integrity. Although the dermal thickness in the P(LA/CL)-HA-nano group was significantly lower than that in the P(LA/CL)-HA group during the second half of the study ($p = 0.0264$), the nanostructured threads continued to demonstrate efficacy and represented a preferable option for application in areas with thin skin.

The skin's extracellular matrix is primarily composed of type I and type III collagen fibers. Type I collagen, a rigid fibrillar protein, accounts for approximately 80%–85% of the dermal matrix and provides mechanical strength and tensile resistance. Type III collagen, which comprises approximately 8–11% of all collagen, forms an elastic reticular network and is crucial for maintaining tissue flexibility, elasticity, and structural integrity [24, 25].

In the P(LA/CL)-HA-nano group, a decrease in type I collagen concentration in the dermal layer was observed from day 7 (80.42 ± 2.18 arbitrary units) to 30 (72.94 ± 3.66); however, this decrease did not reach statistical significance (days 7–21, $p = 0.1380$; days 21–30, $p = 0.5002$).

In contrast, the hypodermal layer exhibited a marked and significant decrease in type I collagen density from day 7 (70.94 ± 4.92) to 21 (21.96 ± 2.94; $p = 0.0431$). This dynamic may reflect a remodeling phase characterized by degradation of pre-existing collagen framework, which may be triggered by mechanical stress or a localized inflammatory response following thread implantation. These changes may be specifically attributed to the biological activity of the nanoencapsulated HA within the threads, distinguishing them from conventional HA formulation used in standard P(LA/CL)-HA threads.

A significant increase in type I collagen density was recorded in the dermal layer from day 30 (72.94 ± 3.66 arbitrary units) to 90 (88.34 ± 1.94; $p = 0.0431$) and in the hypodermal layer from day 21 (21.96 ± 2.94) to 90 (52.76 ± 2.82; $p = 0.0431$), indicating a shift from catabolic to anabolic activity and the onset of an active phase of collagen synthesis. Notably, peak type I collagen density in the dermis was observed on day 90 (88.34 ± 1.94), whereas in the hypodermis, it was reached as early as day 7 (70.94 ± 4.92).

By day 180, type I collagen levels in the dermal (70.46 ± 4.91 arbitrary units) and hypodermal (12.16 ± 0.51) layers had further decreased, returning to values comparable to those in the control (71.12 ± 6.22 in the dermis and 9.20 ± 0.76 in the hypodermis).

Throughout the observation period, the type I collagen density in the hypodermis at the site of P(LA/CL)-HA-nano thread implantation consistently exceeded the control values ($p = 0.00001$), demonstrating a pronounced ability of these threads to stimulate collagen production. A similar trend was not statistically confirmed in the dermis ($p = 0.1829$).

Compared with P(LA/CL)-HA threads, P(LA/CL)-HA-nano threads generally presented lower collagen density in the dermal layer on day 30 (84.82 ± 2.28 vs. 72.94 ± 3.66

arbitrary units; $p = 0.0796$) and in the hypodermal layer on day 21 (43.30 ± 2.75 vs. 21.96 ± 2.94; $p = 0.0431$). An exception was observed on day 7 in the hypodermis, where the collagen density was significantly greater in the P(LA/CL)-HA-nano group (70.94 ± 4.92) than in the P(LA/CL)-HA group (49.91 ± 3.29; $p = 0.0431$). These findings reveal that nanocapsulation may alter the release kinetics or biological activity of HA, potentially affecting its collagen-stimulating capacity compared with conventional HA formulations.

Throughout the observation period, no significant day-to-day fluctuations in type III collagen density were observed in the dermal layer following P(LA/CL)-HA-nano thread implantation (days 7–21: $p = 0.3452$; days 21–30: $p = 0.5002$; days 30–90: $p = 0.8927$; and days 90–180: $p = 0.2249$).

Notably, the present study revealed a significant increase in type III collagen content in the hypodermis between day 7 (17.60 ± 3.65 arbitrary units) and 21 (51.74 ± 2.52; $p = 0.0431$). This increase may reflect active collagen synthesis or restructuring induced by the implantation of threads containing nanoencapsulated HA. A trend toward decreased type III collagen density was subsequently recorded between day 21 (51.74 ± 2.52) and 90 (21.68 ± 1.53; $p = 0.0431$), which indicates a transition from the synthesis phase to the remodeling phase, during which type III collagen is gradually replaced by structurally stronger type I collagen.

By day 180, a secondary increase in type III collagen density was observed, reaching statistical significance in the hypodermis (51.86 ± 0.61 arbitrary units; $p = 0.0431$) and showing a nonsignificant increase in the dermis (8.76 ± 2.09; $p = 0.2249$). These findings may indicate the onset of a secondary phase of collagen accumulation or reactivation of the tissue remodeling processes critical for achieving final morphofunctional stabilization and integration of the threads into the hypodermal matrix.

Throughout the observation period, a trend toward statistical significance was observed in the dermis: the level of type III collagen increased from day 7 (4.84 ± 0.58) to 180 (8.76 ± 2.09; $p = 0.0796$). In contrast, the hypodermal layer presented a significant increase in type III collagen from day 7 (17.60 ± 3.65) to day 180 (51.86 ± 0.61; $p = 0.0431$).

Compared with the control (12.18 ± 2.77 arbitrary units), the use of P(LA/CL)-HA-nano threads was associated with a decreased density of type III collagen in the dermis at most time points. Significant differences were observed on days 7 (4.84 ± 0.58) and 30 (4.06 ± 0.71; $p = 0.0431$), whereas a trend toward significance was noted by day 90 (4.56 ± 1.13; $p = 0.0796$).

However, throughout the study period, the density of type III collagen in the hypoderm was consistently greater than that in the control (13.70 ± 1.18). Significant differences were recorded from day 21 (51.74 ± 2.52) to 180 (51.86 ± 0.61; $p = 0.0431$).

The observed differences in the dermal and hypodermal responses to P(LA/CL)-HA-nano thread implantation, manifested in the divergent dynamics of type III collagen density,

may be associated with variations in the biological environment and functional roles of these skin layers.

The dermis, which is located closer to the surface and actively involved in the early phases of wound healing, may undergo a more rapid remodeling process, during which type III collagen is relatively quickly replaced by mechanically stronger type I collagen. This mechanism may account for the lower type III collagen values in the dermis than in the control.

In contrast, the hypodermis, situated in deeper layers and governed by distinct tissue renewal mechanisms and kinetics, may tend to retain or even accumulate type III collagen. This may reflect a more prolonged recovery process and structural stabilization within the tissue matrix.

Compared with the P(LA/CL)-HA material, P(LA/CL)-HA-nano threads exhibited distinct kinetics in the dermal layer, initially presenting with lower type III collagen levels ($p = 0.0796$). However, by day 180, the values in the nano group exceeded those in the P(LA/CL)-HA group (4.06 ± 0.81 vs. 8.76 ± 2.09 arbitrary units; $p = 0.1380$), although the difference did not reach statistical significance.

In the hypodermal layer, the nanomodified threads consistently induced significantly increased type III collagen levels starting from day 21. On day 21, the collagen level was 24.52 ± 1.87 in the P(LA/CL)-HA group and 51.74 ± 2.52 in the P(LA/CL)-HA-nano group. By day 180, the values reached 30.90 ± 3.29 and 51.86 ± 0.61, respectively.

These findings reveal the potential of nanoencapsulation technology to increase type III collagen deposition within the hypodermis.

Ultimately, P(LA/CL)-HA-nano threads exerted differential effects on type III collagen density in the dermal and hypodermal layers, demonstrating the distinct biological environments and functional roles of these skin compartments. In the dermis, a more rapid remodeling response accompanied by a subsequent decrease in type III collagen levels was observed. Conversely, the hypodermis exhibited a sustained increase in type III collagen content, indicating the involvement of distinct healing and tissue integration mechanisms.

Overall, although both P(LA/CL)-HA and P(LA/CL)-HA-nano threads demonstrated dynamic changes in collagen deposition over time, they exhibited distinctly different patterns. The P(LA/CL)-HA-nano group initially presented higher early levels of collagen, particularly type I collagen in the hypodermis and type III collagen at later stages in the same layer. However, the P(LA/CL)-HA group was characterized by a more stable and prolonged increase in collagen, particularly type I collagen, during the middle to late observation periods. Although many of the intergroup differences did not reach statistical significance, the observed trends show that the nanomodified suture material induces a more rapid but shorter-lived collagen response, whereas the conventional variant supports a more sustained remodeling process.

In the initial days following implantation, no significant changes in elastin content were observed in the dermal layer between day 7 (1.32 ± 0.11 a.u.) and 21 (1.16 ± 0.04 a.u.),

which may indicate early stabilization of the tissue response to thread insertion. Subsequently, up to day 90 (1.70 ± 0.03 a.u.), the dermal structure exhibited a steady state without marked fluctuations in this parameter, revealing gradual adaptation of the tissue to the presence of the biomaterial. By day 90, with a continued trend observed through day 180 (2.08 ± 0.17 a.u.), a pattern of increasing elastin density was recorded ($p = 0.0796$), indicating the potential of the threads to stimulate elastogenesis or promote structural integration of elastin fibers into the dermal matrix over an extended period.

A different pattern was observed in the hypodermal layer following the implantation of P(LA/CL)-HA-nano threads. On day 7, elastin levels in the hypodermis were significantly lower than those in the control (0.18 ± 0.04 a.u. vs. 1.14 ± 0.10 a.u.; $p = 0.0431$), potentially indicating temporary suppression of elastin synthesis or redistribution of tissue resources in response to thread implantation. From day 21 (1.54 ± 0.10 a.u.) to 180 (1.32 ± 0.12 a.u.), the elastin density generally exceeded the control value, with a trend toward statistical significance observed on days 21 and 90 (1.52 ± 0.07 a.u.). However, no significant differences were recorded between these time points. These findings demonstrate recovery and subsequent enhancement of elastin production, possibly mediated by the bioactive properties of the nanothreads, which may stimulate elastin synthesis or modulate its degradation pathways.

P(LA/CL)-HA-nano threads significantly increased elastin density in the dermal and hypodermal layers over the 7- to 180-day observation period. In the dermis, the elastin content increased from 1.32 ± 0.11 a.u. to 2.08 ± 0.17 a.u.; in the hypodermis, it increased from 0.18 ± 0.04 a.u. to 1.32 ± 0.12 a.u. ($p = 0.0431$ for both comparisons). These findings show that P(LA/CL)-HA-nano threads induce a pronounced elastogenic effect.

The use of P(LA/CL)-HA-nano threads resulted in a sustained increase in the elastin content in the dermal layer on days 90 (1.70 ± 0.03 a.u.) and 180 (2.08 ± 0.17 a.u.) than in the control, with significant differences observed ($p = 0.0431$). A similar trend was not observed in the hypodermis; a tendency toward statistical significance was noted only on days 21 (1.54 ± 0.10 a.u.) and 90 (1.52 ± 0.07 a.u.) ($p = 0.0796$).

Compared with P(LA/CL)-HA threads, P(LA/CL)-HA-nano threads elicited distinct elastin-related responses in the dermal layer. This difference was most pronounced on day 21, when the elastin level was significantly greater in the P(LA/CL)-HA group (1.48 ± 0.07 a.u.) than in the P(LA/CL)-HA-nano group (1.16 ± 0.047 a.u.; $p = 0.0431$), potentially indicating differences in tissue interactions or in the regulatory mechanisms governing elastin synthesis. In contrast, on days 7, 90, and 180, elastin concentration was greater in the area of the P(LA/CL)-HA-nano threads than in that of the standard P(LA/CL)-HA threads. Specifically, the values in the P(LA/CL)-HA-nano group were 1.32 ± 0.11 a.u. (day 7), 1.70 ± 0.03 a.u. (day 90), and 2.08 ± 0.17 a.u. (day 180), whereas those in the P(LA/CL)-HA group were 1.18 ± 0.20, 1.44 ± 0.13, and

1.80 ± 0.06 a.u., respectively. However, these differences did not reach statistical significance (day 7, $p = 0.5002$; day 90, $p = 0.1380$; and day 180, $p = 0.1056$).

In the hypodermal layer, the P(LA/CL)-HA-nano material resulted in a significantly lower elastin level than the P(LA/CL)-HA threads did on day 180 (1.32 ± 0.12 a.u. vs. 2.16 ± 0.22 a.u.). Although the elastin levels were consistently lower in the nano-thread group at earlier time points—on days 7 (0.18 ± 0.04 a.u. vs. 0.94 ± 0.27 a.u.), 30 (1.28 ± 0.16 a.u. vs. 1.48 ± 0.16 a.u.), and 90 (1.52 ± 0.07 a.u. vs. 1.56 ±0.04 a.u.)—these differences did not reach statistical significance ($p > 0.05$). These findings indicate that compositional differences between thread types may differentially affect elastin dynamics, possibly due to variations in the release profiles of bioactive agents or physical properties of the threads themselves.

Therefore, this animal model study revealed subtle features of the interaction between the P(LA/CL)-HA-nano thread material and tissue elastin levels over a 6-month observation period. In the early stages (up to day 30) post-implantation, stabilization of elastin content in the dermis indicated that P(LA/CL)-HA-nano threads facilitate gradual tissue adaptation without inducing abrupt structural changes.

The marked increase in elastin density observed on days 90 and 180, particularly in the dermis, demonstrates the prolonged biological effect of the threads, promoting elastogenesis and the integration of elastic fibers into the tissue matrix. Such enhancement of elastin structural organization is crucial in maintaining skin elasticity and architectural integrity, which may contribute to improved aesthetic outcomes and greater longevity of the restored tissues.

CONCLUSIONS

Based on the results of the histomorphological evaluation, P(LA/CL)-HA-nano threads demonstrate efficacy in inducing skin tissue remodeling processes following implantation in a porcine experimental model. The significant increase in dermal thickness along with evidence of the material's capacity to modulate the synthesis of type I and III collagens and prolonged stimulatory effect on elastogenesis emphasize the pronounced bioactive properties of the tested threads and their potential as promising tools for use in aesthetic and reconstructive medicine.

ADDITIONAL INFORMATION

ДОПОЛНИТЕЛЬНАЯ ИНФОРМАЦИЯ

СПИСОК ЛИТЕРАТУРЫ | REFERENCES

1. Li K, Meng F, Li YR, et al. Application of Nonsurgical Modalities in Improving Facial Aging. *Int J Dent*. 2022;2022:8332631. doi: 10.1155/2022/8332631 EDN: HVLNVJ

2. Kochhar A, Kumar P, Karimi K. Minimally Invasive Techniques for Facial Rejuvenation Utilizing Polydioxanone Threads. *Clin Plast Surg*. 2023;50:465–477. doi: 10.1016/j.cps.2022.12.011 EDN: YHLOAJ

3. Borzykh OB, Karpova EI, Shnayder NA, Demina OM. Contemporary View on Thread Lifting: Histological and Anatomical Approaches. *Russian Open Medical Journal*. 2022;11(1):107. doi: 10.15275/rusomj.2022.0107 EDN: PLLTDP

4. Ruff GL. The History of Barbed Sutures. *Aesthet Surg J*. 2013;33(Suppl 12):6S-12S. doi: 10.1177/1090820X13498505

5. Song R, Murphy M, Li C, et al. Current Development of Biodegradable Polymeric Materials for Biomedical Applications. *Drug Des Devel Ther*. 2018;12:3117–3145. doi: 10.2147/DDDT.S165440 EDN: SXISTO

6. Zhang M, Chang Z, Wang X, Li Q. Synthesis of Poly(l-lactide-co-ε-caprolactone) Copolymer: Structure, Toughness, and Elasticity. *Polymers*. 2021;13(8):1270. doi: 10.3390/polym13081270 EDN: ZUQSQU

7. Jelonek K, Kasperczyk J, Li S, et al. Novel poly(L-lactide-co-ε-caprolactone) matrices obtained with the use of Zr[Acac]₄ as nontoxic initiator for long-term release of immunosuppressive drugs. *International BR*. 2013;2013:607351. doi: 10.1155/2013/60735

8. Wong V. The Science of Absorbable Poly(L-Lactide-Co-ε-Caprolactone) Threads for Soft Tissue Repositioning of the Face: An Evidence-Based Evaluation of Their Physical Properties and Clinical Application. *Clin Cosmet Investig Dermatol*. 2021;14:45–54. doi: 10.2147/ccid.s274160 EDN: QHQFII

9. Sulamanidze GM, Sulamanidze MA, Sulamanidze KM, et al. The Subcutaneous Tissue Reaction on Poly (L-lactide-co-caprolactone) Based Threads. *Clin Exp Dermatol*. 2018;3(2):1–9. doi: 10.33140/IJCED

10. Burko P, Miltiadis I. Evolution of Thread Lifting: Advancing Toward Bioactive Polymers and Sustained Hyaluronic Acid Delivery. *Cosmetics*. 2025;12(3):127. doi: 10.3390/cosmetics12030127

11. Liao ZF, Yang W, Li X, et al. Infraorbital Rejuvenation Combined with Thread-Lifting and Non-Cross-Linked Hyaluronic Acid Injection: A Retrospective, Case-Series Study. *Aesthetic Plast Surg*. 2024;48(8):1589–1596. doi: 10.1007/s00266-023-03740-1 EDN: IOZXFF

12. Liao ZF, Yang W, Lin FC, et al. A Case Study: Comprehensive Approach for Treating Horizontal Neck Wrinkles Using Hyaluronic Acid Injections and Thread-Lifting. *Aesthetic Plast Surg*. 2023;47(2):765–771. doi: 10.1007/s00266-022-03071-7 EDN: ACZIOS

13. Yi KH, Kim SB, Hu H, et al. Self-Crossing Hyaluronic Acid Filler with Combination Use of Polydioxanone Thread in Minipig Model. *J Cosmet Dermatol*. 2024;23(9):2821–2828. doi: 10.1111/jocd.16338 EDN: YDTZEB

14. Moon H, Fundaro SP, Goh CL, et al. A Review on the Combined Use of Soft Tissue Filler, Suspension Threads, and Botulinum Toxin for Facial Rejuvenation. *Cutan Aesthet Surg*. 2021;14(2):147. doi: 10.4103/jcas.jcas_119_20 EDN: LLTGKG

15. Niu Z, Zhang K, Yao W, et al. A Meta-Analysis and Systematic Review of the Incidences of Complications Following Facial Thread-Lifting. *Aesthetic Plast Surg*. 2021;45(5):2148–2158. doi: 10.1007/s00266-021-02256-w EDN: HRQPBB

16. Samizadeh S, Samizadeh S. Thread Types and Materials. In: *Thread Lifting Techniques for Facial Rejuvenation and Recontouring*. Samizadeh S, editor. Cham: Springer International Publishing; 2024. P. 179–198. doi: 10.1007/978-3-031-47954-0_8

17. Ziade G, Daou D, Karam D, Tsintsadze M. The Third Generation Barbed Lifting Threads: Added Value of Hyaluronic Acid. *J Cosmet Dermatol*. 2024;23(1):186–192. doi: 10.1111/jocd.15885 EDN: WKNFUL

18. Patent RUS №2782112 C2/ 21.10.2022. IPC A61L 17/10, A61B 17/04. Sulamanidze MA, Nikishin DV, Sulamanidze GM, et al. *Method for production of medical implant shell, medical implant shell*. Applicant: APTOS LLC. EDN: JSOCYJ

19. Burko P, Sulamanidze G, Nikishin D. Long-Term Efficacy of Poly(L-Lactide-Co-ε-Caprolactone) Copolymer Lifting Threads with Encapsulated MICROscale Hyaluronic Acid Particles Using NAMICA Technology: Investigating Biorevitalizing Effects in Skin Remodeling (Part 1). *Cosmetics*. 2025;12(1):20. doi: 10.3390/cosmetics12010020 EDN: SDFXDA

20. Costea R, Ene I, Pavel R. Pig Sedation and Anesthesia for Medical Research. *Animals*. 2023;13(24):3807. doi: 10.3390/ani13243807 EDN: WHHVUK

21. Mavlikeev MO, Arkhipova SS, Chernova ON. Preparation of paraffin sections. In: Mavlikeev MO, Arkhipova SS, Chernova ON, et al. *A short course in histological techniques: a teaching and methodological guide*. Deev RV, editor. Kazan: Kazan University; 2020. 107 p. (In Russ.)

22. Chen LH, Xue JF, Zheng ZY, et al. Hyaluronic acid, an efficient biomacromolecule for treatment of inflammatory skin and joint diseases: A review of recent developments and critical appraisal of preclinical and clinical investigations. *Int J Biol Macromol*. 2018;116:572–584. doi: 10.1016/j.ijbiomac.2018.05.068 EDN: YHTINF

23. Pilloni A, Marini L, Gagliano N, et al. Clinical, histological, immunohistochemical, and biomolecular analysis of hyaluronic acid in early wound healing of human gingival tissues: A randomized, split-mouth trial. *J Periodontol*. 2023;94:868–881. doi: 10.1002/JPER.22-0338 EDN: NWBMMA

24. Dab H, Kacem K, Hachani R, et al. Physiological Regulation of Extracellular Matrix Collagen and Elastin in the Arterial Wall of Rats by Noradrenergic Tone and Angiotensin II. *J Renin Angiotensin Aldosterone Syst*. 2012;13(1):19–28. doi: 10.1177/1470320311414752

25. Davison-Kotler E, Marshall WS, García-Gareta E. Sources of Collagen for Biomaterials in Skin Wound Healing. *Bioengineering*. 2019;6(3):56. doi: 10.3390/bioengineering6030056

AUTHORS INFO

* Pavel A. Burko, MD, MSc, PhD student, Depart. of Biomedicine, Neurosciences and Advanced Diagnostics (BiND), Section of Human Anatomy, University of Palermo;
Senior Lecturer, Faculty of Medicine, Depart. of Biomedical Siences, Moscow University "Synergy";
address: 129 Via del Vespro, Palermo, PA, Italy, 90127;
ORCID: 0000-0002-1344-9654;
eLibrary SPIN: 5673-7871;
e-mail: pavel.burko@unipa.it

George M. Sulamanidze, MD, Cand. Sci. (Medicine),
General Director;
ORCID: 0000-0003-2759-020X;
e-mail: aptos@aptos.ge

Dmitriy V. Nikishin, MD, Cand. Sci. (Medicine), Assistant Professor, Deputy General Director for Research and Development, Russian Office of APTOS;
ORCID: 0000-0002-0959-252X;
eLibrary SPIN: 4424-9565;
e-mail: d.nikishin@aptos.group

ОБ АВТОРАХ

* Бурко Павел Александрович, аспирант, каф. биомедицины, нейронаук и современных методов диагностики (BiND), секция анатомии человека, Университет города Палермо; старший преподаватель, медицинский факультет, каф. медико-биологических дисциплин, Московский университет «Синергия»;
адрес: Италия, 90127, Палермо, провинция Палермо, ул. дель Веспро, д. 129;
ORCID: 0000-0002-1344-9654;
eLibrary SPIN: 5673-7871;
e-mail: pavel.burko@unipa.it

Суламанидзе Георгий Марленович, канд. мед. наук, генеральный директор;
ORCID: 0000-0003-2759-020X;
e-mail: aptos@aptos.ge

Никишин Дмитрий Викторович, канд. мед. наук, доцент, заместитель генерального директора по научным исследованиям и разработкам, Российский офис ООО «АПТОС»;
ORCID: 0000-0002-0959-252X;
eLibrary SPIN: 4424-9565;
e-mail: d.nikishin@aptos.group

* Corresponding author / Автор, ответственный за переписку